Research Square

Preprints are preliminary reports that have not undergone peer review.
They should not be considered conclusive, used to inform clinical practice,
or referenced by the media as validated information.

Outage Analysis and Location Estimation of Cooperative GEO/LEO ISAC Network with Imperfect CSI

Tao Teng
Wuxi University
Lei Kong
Wuxi University
Xuan Yang
Wuxi University
Rongrong Gu
860532@cwxu.edu.cn

Wuxi University

Research Article

Keywords:

Posted Date: November 9th, 2026

DOI: https://doi.org/10.21203/rs.3.rs-11438222/v1

License: This work is licensed under a Creative Commons Attribution 4.0 International License.
Read Full License

Additional Declarations: No competing interests reported.

Outage Analysis and Location Estimation of Cooperative GEO/LEO ISAC Network with Imperfect CSI

Abstract

As the demand for integrated connectivity and wide-area sensing in sixth-generation (6G) non-terrestrial networks, satellite integrated sensing and communication (SAT-ISAC) has attracted increasing attention in recent works. However, due to the limited echo signal power in monostatic GEO satellite ISAC systems, bistatic GEO/LEO satellite ISAC offers enhanced echo signal strength and cooperative communication capabilities, making it a promising research direction. This paper investigates the cooperative target sensing and multi-user communication of a two-layer satellite system with the consideration of imperfect channel state information (CSI). First, we analyze the detection probability of sensing signal and the outage probability (OP) of terrestrial user terminals (UTs). Besides, the asymptotic OP is derived to characterize the communication performance in the high signal-to-noise ratio (SNR) region. To enhance sensing performance, a statistical detection probability maximization problem is proposed, while ensuring OP constraint, a successive convex approximation (SCA) based beamforming design strategy is proposed . Additionally, the target location estimation is introduced, leveraging the advantages of cooperative GEO/LEO network to estimate the delay and angle information. The Crameŕ-Rao Bound (CRB) is also derived as a low bound on the mean square error of the parameter estimates. Finally, we validate the theoretical findings through Monte Carlo simulations, which demonstrate that the proposed beamforming algorithm can effectively support target sensing tasks. The optimization results show that the proposed algorithm achieves superior performance.

Keywords: Integrated sensing and communication, GEO/LEO network, imperfect CSI, delay and angle estimation

1 Introduction

Integrated sensing and communication (ISAC) systems exploit shared spectrum resources for both radar sensing and wireless communication, offering a promising approach to improving spectrum utilization while balancing communication and sensing performance [1, 2]. Recent studies have extensively investigated terrestrial ISAC system, including cell-free ISAC systems [3], UAV-assisted ISAC systems [4], and

reconfigurable intelligent surfaces (RIS) assisted ISAC systems [5]. Optical Wireless ISAC (ISAC-OW) technologies have also been explored at the One6G Summit, where visible light and infrared spectra are investigated for applications in healthcare, robotics, and smart hospitals. However, achieving effective and low-latency communication through a single satellite layer remains challenging. These challenges require the careful consideration of the multi-layer satellite architectures [6].

Most existing SAT-ISAC studies have primarily focused on single-layer architectures, specifically the Low Earth Orbit (LEO) satellite networks. For example, authors in [7, 8] have investigated energy efficiency optimization in massive multiple-input multiple-output (MIMO)-enabled LEO SAT-ISAC networks, accounting for beam squint effects and sensing beampattern constraints. Similarly, authors in [9] focused on energy efficiency in single-layer LEO satellite systems using the Crameŕ-Rao Bound (CRB) to characterize sensing performance. Despite these advances, single-layer LEO systems may experience limited target observation and time-varying geometry due to orbital motion. Nevertheless, LEO monostatic radar systems face challenges like long revisit times and limited coverage due to the high-speed motion of these satellites. As a result, Geostationary Earth Orbit (GEO)/LEO bistatic radar (biSAR) systems [10, 11] have been proposed to enable more comprehensive terrestrial surveillance and improve the flexibility of radar signal reception.

Motivated by these considerations, this work investigates detection performance and interference management in a two-layer GEO/LEO SAT-ISAC system. Specifically, the GEO satellite transmits a sensing signals, while the LEO satellite captures the targt echo signal, forming a bistatic sensing framework. This architecture separates the sensing transmitter and receiver, and provides additional flexibility in sensing geometry compared with a monostatic system. To address the communication and sensing problem, we propose a two-stage framework. In the first stage, the communication and sensing performance metrics are analyzed, and an optimization problem is formulated to enhance the cooperative sensing performance. In the second stage, the communication and sensing performance metrics are analyzed, and an optimization problem is formulated to improve the sensing performance. The main contributions of this paper are summarized as follows:

- We consider a cooperative GEO/LEO SAT-ISAC system with imperfect CSI, in which the GEO satellite transmits the sensing waveform and the LEO satellite receives the target echo. We first analyze the detection probability based on the target reflection power, and then the outage probability (OP) is evaluated to characterize the reliability of delay-sensitive satellite transmission. The asymptotic OP is also calculated in the high signal-noise-ratio (SNR) regime. Furthermore, we formulate a statistical optimization problem to maximize the detection probability while subject to the multi-user OP constraints. The successive convex approximation (SCA)-based beamforming algorithm is proposed to solve the non-convex problem.
- In the second stage, the LEO SAT perform target tracking by estimating both the signal delay and angle of arrival from the received echoes. Combined with the known geometric locations of the satellites, the target position can be determined, and the corresponding CRB is derived as a theoretical lower bound to assess the mean square error (MSE) of parameters.

- Monte Carlo simulations have been conducted to verify the theoretical expressions. Furthermore, the detection probability optimization across different beamforming benchmarks is shown. Simulation results also highlight the accuracy of the target location estimation compared with the CRB.

2 Related Works

2.1 The advantage of the Bistatic System

Integrated Sensing and Communication (ISAC) has advanced considerably over the past decade, where both sensing and communication functions are performed by a single target. Recent developments have shifted towards bistatic ISAC systems, where transmitters and receivers are spatially separated, which provides greater spatial diversity and expanded sensing coverage.

In [12], the authors investigated a bistatic ISAC system with orthogonal frequency-division multiplexing (OFDM). The authors showed that the bistatic configuration outperforms the monostatic one because the base station does not need to operate in full-duplex mode, which reducing self-interference. In addition, the bistatic framework brings the flexibility for network architecture design. In [13], the authors derived a coordinated beamforming (CBF) scheme for bistatic sensing in multi-cell scenarios and compared it with monostatic sensing. Different from traditional monostatic GEO SAT systems, the GEO/LEO bistatic network offers a significantly improved echo power ratio, with approximately 64 times higher received echo power [10].

2.2 GEO-LEO Coexistence and Interference System

GEO satellites, with their fixed position relative to Earth, provide continuous communication services, making them suitable for long-term monitoring and broadcast services. In contrast, LEO satellites, closer to Earth, offer lower latency, higher data throughput, and flexible networking, although they require more dynamic resource management. The coexistence of GEO and LEO satellites in multi-layered networks enables robust communication systems that combine the strengths of both layers.

However, this setup introduces co-channel interference, as GEO and LEO satellites share time-frequency resources, which degrades the communication performance of both system. Consequently, inter-system interference management becomes a critical design challenge, requiring careful resource optimization to fully leverage the advantages of GEO-LEO networks. In [14], a joint beam-management and power-allocation (JBMPA) scheme was proposed to maximize signal-to-interference plus noise ratio (SINR) at the GEO user to decrease the interference caused by LEO. To address the interference caused by the increasing number of satellite and limited frequency bands, the authors in [15] proposed a flexible spectrum sharing and cooperative service method to overcome the co-linear interference issue caused by the coverage area of a GEO beam.

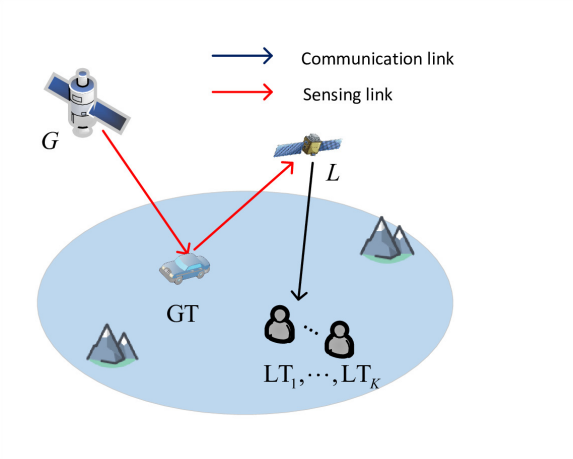


Fig. 1 Integrated sensing and communications for two-layer GEO/LEO satellite system.

2.3 GEO-LEO Satellite Coexistence ISAC System

Combining sensing and communication capabilities in these satellite networks presents unique challenges, particularly in managing interference arising from shared resources across multiple orbital layers. Recent studies have focused on advanced signal processing techniques, including rate-splitting multiple access (RSMA) and beamforming optimizations, to efficiently support the dual functionality of LEO satellite efficiently.

Authors in [16] utilized RSMA to manage the multi-user interference and formulated a max-min fairness energy efficiency (EE) optimization problem for an RSMA-assisted LEO satellite ISAC system under the limited power. Moreover, as illustrated in [17], the LEO ISAC systems require efficient spectrum and hardware utilization to cope with severe electromagnetic spectrum congestion, which benefits from the ability to suppress interference achieving an improved communication sensing tradeoff.

3 System Model

As illustrated in Fig.1, a Ka-band two-tier satellite network is considered, comprising both GEO and LEO satellites as well as multiple user terminals (UTs). The satellites operate on shared time-frequency resources and are managed by ground-based gateways via feeder links, the gateways handle signal processing and power control. The GEO SAT is equipped with N_G uniform linear array (ULA) antennas, which serve a single GEO terminal (GT). Moreover, the LEO SAT has N_L ULA antennas, which offers unicast communication to K LEO terminals (LTs) [18]. The GT and all LTs are equipped with a single antenna.

We assumed that the GEO SAT has the radar signal transmission capabilities. The proposed two-stage SAT-ISAC operates as follows: 1) In the first stage, the GEO SAT transmits the radar signal for target tracking, and the LEO SAT transmits the unicast signals simultaneously. 2) In the second stage, the LEO SAT provides coordinate

estimation towards the target, which is then shared with the GEO satellite to provide cooperative communication service. Let $\mathbf{q}_r = [q_r^x, q_r^y, q_r^z], \mathbf{q}_G = [q_G^x, q_G^y, q_G^z], \mathbf{q}_L = [q_L^x, q_L^y, q_L^z]$ represent the position of the target, GEO, and LEO SAT, respectively. The downlink transmission signal from the two-tier satellite system at time $t, t \in \{1, \cdots, T\}$ can be expressed as follows:

$$\mathbf{x}_G(t) = \sqrt{p_G}\mathbf{w}_{G,r}x_{G,r}(t), \tag{1}$$

and

$$\mathbf{x}_L(t) = \sqrt{p_L}\sum_{k=1}^{K}\mathbf{w}_{L,k}x_{L,k}(t), \tag{2}$$

where p_G and p_L denote the transmitting power. $\mathbf{w}_{G,r} \in \mathbb{C}^{N_G \times 1}$, $\mathbf{w}_{L,k} \in \mathbb{C}^{N_L \times 1}$ denote the transmitting beamforming of the GEO and LEO SAT, which satisfy $\sum_{k=1}^{K}\|\mathbf{w}_{L,k}\|^2 = 1$. Specifically, the sensing signal and communication signal are mutually independent [19]. The communication signal satisfies $\mathbb{E}\left\{|x_{L,k}|^2\right\} = 1$ for $k \in \{1, \cdots, K\}$. Then, the coherent covariance matrix of the transmitted signals can be calculated as $\mathbf{R}_G = p_G\mathbf{w}_r\mathbf{w}_r^H$, and $\mathbf{R}_L = p_L\sum_{k=1}^{K}\mathbf{w}_{L,k}\mathbf{w}_{L,k}^H$.

3.1 Communication Signal Receiver Model

Due to the large distance between GEO SAT (at the altitude 36000km) and terrestrial receivers , the channel fading from the GEO to $i \in \{r, 1, \cdots, K\}$ is modeled as the shadowed-Rician fading with parameters $(b_{G,i}, m_{G,i}, \Omega_{G,i})$ [20], where $i = r$ denotes the GT and $i \in \{1, \cdots, K\}$ is the K LTs. Define $\mathbf{a}(\theta_{G,i}) = \frac{1}{\sqrt{N_G}}\left[1, e^{j\frac{2\pi}{\lambda}d_{G,i}\sin\theta_{G,i}}, \cdots, e^{j\frac{2\pi}{\lambda}d_{G,i}(N_G-1)\sin\theta_{G,i}}\right]^T$. In practice, perfect CSI is difficult to obtain because of channel estimation errors (CEEs)[21], therefore, $\mathbf{h}_{G,i}$ can be formulated as follows

$$\mathbf{h}_{G,i} = \sqrt{\chi_{G,i}}\widehat{g}_{G,i}\mathbf{a}(\theta_{G,i}) + \mathbf{e}_{G,i} \tag{3}$$

where the estimation error $\tilde{\mathbf{e}}_{G,i}$ follows $\mathcal{CN}\left(0, \sigma_{e_{G,i}}^2\mathbf{I}_{N_G}\right)$, $\sigma_{e_{G,i}}^2$ is determined by the SNR-dependent variance [22].

Note that the propagation gain $\chi_{G,i}$ between the GEO and LEO satellites to the GT and LTs also influence the communication quality, which includes the free space loss and the antenna gain. According to the ITU-R [23], $\chi_{G,i}$ is expressed as

$$\chi_{G,i} = \frac{\sqrt{A_{G,i}}}{4\pi\frac{d_{G,i}}{\lambda}\sqrt{\mathcal{H}\mathcal{T}\mathcal{B}}}, \tag{4}$$

where $A_{G,i}$ is the transmitter-receiver antenna gain, $d_{G,i}$ is the line-of-sight (LoS) propagation distance. λ denotes the carrier wavelength, $\mathcal{B}$ is the bandwidth in Hertz,

$\mathcal{T}$ is the thermal noise, and $\mathcal{H}$ denotes the Boltzmann constant [24]. With a similar approach, the propagation gain for the LEO SAT is given by $\chi_{L,i} = \frac{\sqrt{A_{L,i}}}{4\pi \frac{d_{L,i}}{\lambda}\sqrt{\mathcal{HTB}}}$.

Define $\mathbf{h}_{L,i}$ represents the channel fading of the LEO SAT. Because the satellite moves at high orbital velocity at altitudes between 200 and 2000 km, the channel experiences significant Doppler shifts. The channel fading of LEO SAT is modeled as [8]

$$\mathbf{h}_{L,i} = \sqrt{\chi_{L,i}}\left(\widehat{g}_{L,i} \mathrm{e}^{j2\pi\left(tv_{L,i} - f_c\tau_{L,i}^{\min}\right)}\mathbf{a}\left(\theta_{L,i}\right)\right) + \mathbf{e}_{L,i}, \tag{5}$$

where $\widehat{g}_{L,i}$ is modeled as Rician channel with parameters $(\kappa_{L,i}, \Omega_{L,i})$, and CEE $\tilde{\mathbf{e}}_{L,i}$ is modeled as a $\mathcal{CN}\left(0, \sigma_{e_{L,i}}^2 \mathbf{I}_{N_L}\right)$. $\mathbf{a}\left(\theta_{L,i}\right)$ is set as $\mathbf{a}\left(\theta_{L,i}\right) = \frac{1}{\sqrt{N_L}}\left[1, e^{j\frac{2\pi}{\lambda}d_{L,i}\sin\theta_{L,i}}, \cdots, e^{j\frac{2\pi}{\lambda}d_{L,i}(N_L-1)\sin\theta_{L,i}}\right]^T$. Here, $v_{L,i}$ is the Doppler frequency due to the mobility of the LEO SAT and terminals, and $\tau_{L,i}^{\min}$ represents the minimum delay between LEO satellite and LT.

The signals received at the LT k are composed of the GEO SAT ISAC signal and the LEO SAT signal, which can be expressed as follows:

$$\begin{aligned} y_k(t) = & \underbrace{\sqrt{p_L}\widehat{\mathbf{h}}_{L,k}^H \mathbf{w}_{L,k} x_{L,k}(t)}_{\texttt{desired signal}} + \underbrace{\sqrt{p_L}\mathbf{e}_{L,k}^H \mathbf{w}_{L,k} x_{L,k}(t)}_{\texttt{imperfect CSI interference}} \\ & + \underbrace{\left(\widehat{\mathbf{h}}_{L,k}^H + \mathbf{e}_{L,k}^H\right)\left(\sqrt{p_L}\sum_{j=1,j\neq k}^{K}\mathbf{w}_{L,j}x_{L,j}(t)\right)}_{\texttt{Inter-user interference}} + \\ & \underbrace{\sqrt{p_G}\left(\mathbf{h}_{G,k}^H + \widehat{\mathbf{e}}_{G,k}^H\right)\mathbf{w}_{G,r}x_{G,r}(t)}_{\texttt{GEO interference}} + \underbrace{n_k(t)}_{\texttt{AWGN}}, \end{aligned} \tag{6}$$

where $n_k \sim CN\left(0, \sigma_k^2\right)$ denotes the additive white Gaussian noise (AWGN) at the LT k with variance σ_k^2. Besides, $\widehat{\mathbf{h}}_{L,k} = \sqrt{\chi_{L,k}}\widehat{g}_{L,k}\mathbf{a}\left(\theta_{L,k}\right)\mathrm{e}^{j2\pi\left(tv_{L,k} - f_c\tau_{L,k}^{\min}\right)}$, $\widehat{\mathbf{h}}_{G,k} = \sqrt{\chi_{G,i}}\widehat{g}_{G,i}\mathbf{a}\left(\theta_{G,i}\right)$.

3.2 Echo Signal Receiving Model

The two-tier cooperative SAT network is utilized for target tracking. As is depicted in Fig.1, we denote $\theta_{G,r}$ and $\theta_{L,r}$ as the angle of departure (AoD) of the GEO and LEO SAT relative to the radar target, respectively. The detailed estimation of angles is detailed in the next section. Assuming that radar sequence length is M, in the sensing space [25], the radar echo at LEO SAT of the l-th antenna can be written as

$$\begin{aligned} \mathbf{y}_{L,l} = & \frac{a_{G,r,L}}{\sqrt{N_L}} e^{j\frac{2\pi}{\lambda}d_{L,r}l\sin\theta_{L,r}} e^{j2\pi f_d\tau_1}\mathbf{a}^H\left(\theta_{G,r}\right)\mathbf{x}_G + \\ & \frac{a_{r,r,L}}{\sqrt{N_L}} e^{j\frac{2\pi}{\lambda}d_{L,r}l\sin\theta_{L,r}} e^{j2\pi f_d\tau_2}\mathbf{a}^H\left(\theta_{L,r}\right)\mathbf{x}_L + \mathbf{n}_{L,l} \end{aligned}, \tag{7}$$

where $\mathbf{y}_{L,l}\mathbb{C}^{1\times M}$. τ_1, τ_2 denotes the propagation delay, which is expressed as $\tau_1 = \frac{d_{G,r}+d_{L,r}}{c}, \tau_2 = \frac{2d_{L,r}}{c}$, c denotes the light speed. The radar reflection coefficient from the

GEO-target-LEO is given by $a_{G,r,L} = \frac{\sqrt{A_{G,r}A_{L,r}\sigma_{\mathrm{RCS}}}}{4\pi\frac{d_{G,r}}{\lambda}\frac{d_{r,L}}{\lambda}}$[26], which encompass path loss $d_{G,r}$, $d_{r,L}$, and the target's complex radar cross-section σ_{RCS}. Here, σ_{RCS} represents the strength of the reflected radar signal from the target, which is related to the shape and material of the target. Furthermore, $a_{L,r,L} = \frac{\sqrt{(A_{L,r})^2\sigma_{\mathrm{RCS}}}}{4\pi\left(\frac{d_{L,r}}{\lambda}\right)^2}$. $f_d = f_c\frac{v_{L,r}}{c}$. $\mathbf{n}_L \sim CN\left(0, \sigma_L^2\mathbf{I}_{N_L}\right)$ is the AWGN.

The first term of the right hand of (7) is the sensing signal through target reflection, which is expressed as the round-trip propagation between GEO-target-LEO, and the second term corresponding to the LEO communication signal are reflected by the target and then received by the LEO satellite.

Remark 1: In general, the LEO SAT communication signal is not only used for unicast communication but also plays a role in target sensing [27]. This is because the reflected signal $\mathbf{x}_L$ is known by the LEO SAT, therefore the bistatic receiving radar can estimate the target location with $\mathbf{x}_L$ and $x_{G,r}$ either. Additionally, it can be observed that the target must be within the coverage area of the LEO SAT for the radar reflection echo receiving.

Remark 2: Note that the AoD from the GEO satellite to a terrestrial terminal is almost identical to that to the target, since the GEO-Earth distance (36,000 km) is much larger than the terrestrial coverage radius. For a coverage radius of 350 km, the AoD difference is at most 1, which is far below the angular resolution of the GEO array. The GEO AoD therefore cannot be used directly for localization, and we rely on the LEO-side delay and angle estimates instead.

4 Outage Probability and Detection Probability Analysis

In delay-limited SAT-ISAC, outage probability (OP) is often used to evaluate the system communication reliability. Besides, for the cooperative bistatic ISAC, the detection probability is utilized to characterize the radar detection performance. In the following, we analyze the radar echo signal-to-noise ratio (SNR) and derive the communication receiving SINR. Additionally, the asymptotic OP is derived under high SNR conditions.

4.1 Echo SINR Analysis

For target detection, let $\mathbf{y}_{L,l} \in {}^{1\times M}$ be the vector. The binary hypothesis [28] of the received signal at the LEO SAT, where $\mathcal{H}_0$ and $\mathcal{H}_1$ denotes the absence and the presence of the target, respectively. It can be expressed as

$$\mathbf{y}_{W,l} = \begin{cases} \mathbf{n}_{L,l} & \mathcal{H}_0 \\ \mathbf{y}_{L,l} & \mathcal{H}_1 \end{cases} \tag{8}$$

where the hypothesis $\mathcal{H}_0$ indicates that the target is outside the coverage area of the LEO satellite, or the echo is too weak to be detected, while $\mathcal{H}_1$ denotes that the target is located within the LEO satellite coverage area or the echo signal can be received at

the LEO SAT. It is worth noticing that $a_{G,r,L}$,and $a_{r,r,L}$ consist of the radar reflection coefficient σ_{RCS}, which obeys $\sigma_{\mathrm{RCS}} \sim \mathcal{CN}(0,1)$. By introducing detection threshold ζ, the optimal radiometer detection is given as

$$\frac{1}{N_L}\sum_{l=1}^{N_L}\left\|\mathbf{y}_{W,l}\right\|^2 \gtrless \zeta. \tag{9}$$

In the reflection link, the miss detection probability of the echo from the two propagation links is defined as the γ_r is below the given threshold ζ, denoted as P_{MD}. Using the Neyman-Pearson detector, P_{MD} can be calculated as

$$\begin{aligned} P_{\mathrm{MD}} &= \Pr\left\{\tfrac{1}{N_L}\sum_{l=1}^{N_L}\left(E_l+\sigma_L^2\right)\chi_2^2 \le \zeta\right\} \\ &= 1-e^{-\frac{\zeta}{2\left(E_l+\sigma_L^2\right)}}, \end{aligned} \tag{10}$$

where $E_l = \frac{A_{G,r}A_{L,r}\lambda^2}{16\pi^2 N_L d_{G,r}^2 d_{L,r}^2}\left\|\mathbf{a}^H\left(\theta_{G,r}\right)\mathbf{x}_G\right\|^2 + \frac{A_{L,r}^2\lambda^2}{16\pi^2 N_L d_{L,r}^4}\left\|\mathbf{a}^H\left(\theta_{L,r}\right)\mathbf{x}_L\right\|^2$ for $l \in \{1,\cdots,N_L\}$. Notably that ζ is chosen to guarantee the radar sensing from miss detection, otherwise the system performance would deteriorate. Thus, with the predefined P_{MD}, ζ is given as

$$\zeta = -2\left(E_l+\sigma_L^2\right)\ln\left(1-P_{\mathrm{MD}}\right). \tag{11}$$

As is illustrated in *Remark 2*, because of the large distance between the GEO SAT and the terrestrial terminals, we have $p_G\left\|\mathbf{a}\left(\theta_{G,r}\right)\mathbf{w}_{G,r}\right\|^2 \approx p_G$. On the other hand, the locations of the LTs are assumed to be perfectly known at the receiving LEO SAT, based on the statistical beamforming vectors $\mathbf{w}_{L,k}$, for $k \in \{1,\cdots,K\}$. In the following, a detection probability maximization problem is proposed. Since increasing ζ can be transformed as maximizing the echo SINR. Herein, the echo SINR is given by

$$\gamma_r = p_G\varphi_r + p_L\sum_{j=1}^{K}\varphi_j, \tag{12}$$

where the variables $\varphi_r = \frac{A_{G,r}A_{L,r}\lambda^2}{16\pi^2 N_L d_{G,r}^2 d_{L,r}^2}$, and $\varphi_j = \frac{A_{L,r}^2\lambda^2}{16\pi^2 N_L d_{L,r}^4}\left\|\mathbf{a}^H\left(\theta_{L,r}\right)\mathbf{w}_j\right\|^2$.

4.2 Communication Outage Probability Analysis

Based on the receiving formula in (6), we can derive the SINR at the LT k. The instantaneous SINR of the k-th LT, is given by:

$$\gamma_k = \frac{p_L\left|\widehat{\mathbf{h}}_{L,k}^H\mathbf{w}_{L,k}\right|^2}{p_L\sum\limits_{j=1,j\neq k}^{K}\left|\widehat{\mathbf{h}}_{L,k}^H\mathbf{w}_{L,j}\right|^2 + p_G\left|\mathbf{h}_{G,k}^H\mathbf{w}_{G,r}\right|^2 + \Xi_k}, \tag{13}$$

where $\Xi_k = p_L\left|\mathbf{e}_{L,k}^H\mathbf{w}_{L,k}\right|^2 + p_L\sum\limits_{j=1,j\neq k}^{K}\left|\mathbf{e}_{L,k}^H\mathbf{w}_{L,j}\right|^2 + p_G\left|\widehat{\mathbf{e}}_{G,k}^H\mathbf{w}_{G,r}\right|^2 + \sigma_k^2$ is the interference-plus noise, including the CEE and AWGN.

Given the stochastic nature of the wireless channel of the SR distribution [29], the closed-form CDF of $\left|\widehat{g}_{G,i}\right|^2$ is shown as

$$\begin{aligned} &F_{\left|\widehat{g}_{G,i}\right|^2}(x) = 1 - \sum_{m=0}^{m_{G,i}-1}\binom{m_{G,i}-1}{m}\frac{\alpha_{G,i}\delta_{G,i}^m}{(\beta_{G,i}-\delta_{G,i})^{m+1}}\times \\ &e^{-\frac{(\beta_{G,i}-\delta_{G,i})}{\rho_{G,i}}x}\sum_{n=0}^{m}\frac{1}{n!}\left(\frac{\beta_{G,i}-\delta_{G,i}}{\rho_{G,i}}\right)^n x^n, \end{aligned} \tag{14}$$

where $\rho_{G,i} = 1 - \frac{\sigma_{e_{G,i}}^2}{\mu_{G,i}\chi_{G,i}}$ is the channel estimation coefficient, and $\mu_{G,i} = 2b_{G,i}{}_2F_1\left(-1, m_{G,i}, 1, -\frac{\Omega_{G,i}}{m_{G,i}}\right)$ is the second-order moment of $|g_{G,i}|^2$. Meanwhile, $\left|\widehat{h}_{L,i}\right|^2$ follows Rician distribution and is expressed as

$$\begin{aligned} &f_{\left|\widehat{h}_{L,i}\right|^2}(x) = \frac{1+\kappa_{L,i}}{\rho_{L,i}\Omega_{L,i}}e^{-\frac{1+\kappa_{L,i}}{\rho_{L,i}\Omega_{L,i}}x-\kappa_{L,i}}\times \\ &I_0\left(\sqrt{\frac{4\kappa_{L,i}(\kappa_{L,i}+1)}{\rho_{L,i}\Omega_{L,i}}x}\right), \end{aligned} \tag{15}$$

where $\rho_{L,i} = 1 - \frac{\sigma_{e_{L,i}}^2}{\Omega_{L,i}\chi_{L,i}}$.

By substituting $\mathbf{w}_{G,r}, \mathbf{w}_{L,k}$ into (13), the SINR of LT k for the communication link can be given by

$$\gamma_k = \frac{p_L\phi_{L,k}\left|\widehat{g}_{L,k}\right|^2}{p_L\left|\widehat{g}_{L,k}\right|^2\sum\limits_{j=1,j\neq k}^{K}\phi_{L,j} + p_G\left|\widehat{g}_{G,k}\right|^2\phi_{G,k} + \Xi_k}, \tag{16}$$

where Ξ_k can also be simplified as $\Xi_k = p_L\sigma_{e_{L,k}}^2 + p_L\sum\limits_{j=1,j\neq k}^{K}\sigma_{e_{L,k}}^2 + p_G\sigma_{e_{G,k}}^2 + \sigma_k^2$. The variables $\phi_{G,k} = \chi_{G,k}$, and $\phi_{L,j} = \chi_{L,k}\left|\mathbf{a}^H(\theta_{L,k})\mathbf{w}_{L,j}\right|^2$.

Therefore, the outage probability of the LT k is calculated as

$$P_{out,k} = \Pr\left\{\left|\widehat{g}_{L,k}\right|^2 < \frac{\Gamma_k\left[p_G\left|\widehat{g}_{G,k}\right|^2\phi_{G,k}+\Xi_k\right]}{p_L\left(\phi_{L,k}-\Gamma_k\sum\limits_{j=1,j\neq k}^{K}\phi_{L,j}\right)}\right\}$$
$$= \sum_{s=0}^{\infty}\frac{\kappa_{L,k}^s e^{-\kappa_{L,k}}}{(s!)}\left(1-\sum_{n=0}^{s}\sum_{m=0}^{m_s-1}\frac{C_k}{B_k^{m+n+1}}\times \left(\frac{\Gamma_k p_G\phi_{G,k}}{p_L\left(\phi_{L,k}-\Gamma_k\sum\limits_{j=1,j\neq k}^{K}\phi_{L,j}\right)}\right)^n\right), \quad (17)$$

where $\frac{\phi_{L,k}}{\sum\limits_{j=1,j\neq k}^{K}\phi_{L,j}} > \Gamma_k$, otherwise $P_{out,k} = 1$. The Marcum-Q function can be calculated with the aid of [30, eq.(8.352.1)]. The channel fading parameter is given by $C_k = \frac{(1+\kappa_{L,i})^n}{n!\rho_{L,k}^n}\binom{m_{G,k}-1}{m}\frac{\alpha_{G,k}\delta_{G,k}^m}{m!\rho_{G,k}^{m+1}}\Gamma(m+n+1)$. Besides, $B_k = \frac{(1+\kappa_{L,i})}{\rho_{L,k}}\frac{\Gamma_k p_G\phi_{G,k}}{p_L\left(\phi_{L,k}-\Gamma_k\sum\limits_{j=1,j\neq k}^{K}\phi_{L,j}\right)} + \frac{\beta_{G,i}-\delta_{G,i}}{\rho_{G,k}}$.

It can be found that OP is influenced by B_k and $\frac{\Gamma_k p_G\phi_{G,k}}{p_L\left(\phi_{L,k}-\Gamma_k\sum\limits_{j=1,j\neq k}^{K}\phi_{L,j}\right)}$. However, the closed-form outage probability is mathematically intractable and computationally complex to evaluate, making it difficult to characterize the relationship between B_k and $P_{out,k}$. In this work, we derive the theoretical expressions for the asymptotic OP at high SNR values, which is given as

$$P_{out,k}^{asy} = \frac{(1+\kappa_{L,i})\,e^{-\kappa_{L,i}}}{\rho_{L,i}}\frac{\Gamma_k\left(p_G\mu_{G,k}\phi_{G,r}+\Xi_k\right)}{p_L\left(\phi_{L,k}-\Gamma_k\sum\limits_{j=1,j\neq k}^{K}\phi_{L,j}\right)}, \quad (18)$$

Proof: Firstly, the approximation of $F_{\left|\widehat{g}_{L,i}\right|^2}(x)$ can be derived as $F_{\left|\widehat{g}_{L,k}\right|^2}^{asy}(x) = e^{-\kappa_{L,k}}\left(1-e^{-\frac{(1+\kappa_{L,k})}{\rho_{L,k}}x}\right)$. Then, by applying $1-e^{-x}\approx x$ when $x\to 0$, we have $F_{\left|\widehat{g}_{L,k}\right|^2}^{asy}(x) = e^{-\kappa_{L,k}}\frac{(1+\kappa_{L,k})}{\rho_{L,k}}x$. Substituting $F_{\left|\widehat{g}_{L,k}\right|^2}^{asy}(x)$ into the calculation of $P_{out,k}^{asy}$, the closed-form asymptotic probability can be calculated as (18).

4.3 Problem Formulation and Optimization

The main objective for the LEO sensing satellite system is to maximize the detection probability ζ , while simultaneously meeting the delay-limited communication outage

probability requirements. This optimization problem can be formulated as follows:

$$\max_{p_G,\mathbf{w}_{L,1},\cdots,\mathbf{w}_{L,K}} \zeta \tag{19}$$

$$\text{s.t.} \quad P_{out,k}^{asy} \leq \varepsilon_k, k = 1, ..., K, \tag{c1}$$

$$\sum_{j=1}^{K} \|\mathbf{w}_{L,j}\|^2 \leq 1, \tag{c2}$$

where the optimization goal is to maximize the detection probability. The constraint C1 ensures that the asymptotic outage probability does not exceed a specified threshold ε_k. Based on the analysis in (12), maximizing ζ can be transformed into an equivalent problem of maximizing the echo SINR. It can be found that the asymptotic OP increases monotonically as $\frac{\Gamma_k(p_G\mu_{G,k}\phi_{G,r}+\Xi_k)}{p_L\left(\phi_{L,k}-\Gamma_k\sum\limits_{j=1,j\neq k}^{K}\phi_{L,j}\right)}$ improves. C1 for $k \in \{1, \cdots, K\}$ can be transformed into

$$p_L\left(\left\|\mathbf{a}^H\left(\theta_{L,k}\right)\mathbf{w}_{L,k}\right\|^2 - \Gamma_k\sum_{j=1,j\neq k}^{K}\beta_{L,j}\left\|\mathbf{a}^H\left(\theta_{L,k}\right)\mathbf{w}_{L,j}\right\|^2\right) \geq \frac{(1+\kappa_{L,i})e^{-\kappa_{L,i}\Gamma_k}}{\rho_{L,i}\varepsilon_k}\left(p_G\mu_{G,k}\phi_{G,r}+\Xi_k\right), \tag{20}$$

and

$$\left\|\mathbf{a}^H\left(\theta_{L,k}\right)\mathbf{w}_{L,k}\right\|^2 - \Gamma_k\sum_{j=1,j\neq k}^{K}\left\|\mathbf{a}^H\left(\theta_{L,k}\right)\mathbf{w}_{L,j}\right\|^2 > 0, \tag{21}$$

To handle the non-convexity of the optimization problem, we develop an SCA-based beamforming approach. Specifically, the non-convexity of (20) and (21)arises from the convex quadratic terms $\|\mathbf{a}\left(\theta_{L,r}\right)\mathbf{w}_{L,k}\|^2, \|\mathbf{a}\left(\theta_{L,k}\right)\mathbf{w}_{L,k}\|^2$. Besides, we utilize the SCA-based algorithm, and introduce the auxiliary variables $y_k = \|\mathbf{a}\left(\theta_{L,r}\right)\mathbf{w}_{L,k}\|^2$ as well as $z_k = \|\mathbf{a}\left(\theta_{L,k}\right)\mathbf{w}_{L,k}\|^2$. By approximating the non-convex terms using their first-order Taylor expansions at the i-th iteration, the expressions of (20) and (21 can be transformed as

$$p_L\left(z_k - \Gamma_k\sum_{j=1,j\neq k}^{K}\beta_{L,j}\left\|\mathbf{a}^H\left(\theta_{L,k}\right)\mathbf{w}_{L,j}\right\|^2\right) \geq \frac{(1+\kappa_{L,i})e^{-\kappa_{L,i}\Gamma_k}}{\rho_{L,i}\varepsilon_k}\left(p_G\mu_{G,k}\phi_{G,r}+\Xi_k\right) \tag{22}$$

$$z_k - \Gamma_k\sum_{j=1,j\neq k}^{K}\left\|\mathbf{a}^H\left(\theta_{L,k}\right)\mathbf{w}_{L,j}\right\|^2 > 0 \tag{23}$$

$$z_k \geq 2\text{Re}\left\{\mathbf{w}_{L,k}\mathbf{a}\left(\theta_{L,k}\right)\mathbf{a}^H\left(\theta_{L,k}\right)\mathbf{w}_{L,k}^{(i-1)}\right\} \tag{24}$$

In addition, $\left\|\mathbf{a}^H\left(\theta_{L,r}\right)\mathbf{w}_{L,j}\right\|^2$ can be rewritten as

$$y_j \geq 2\text{Re}\left\{\mathbf{w}_{L,j}\mathbf{a}\left(\theta_{L,r}\right)\mathbf{a}^H\left(\theta_{L,r}\right)\mathbf{w}_{L,j}^{(i-1)}\right\} \tag{25}$$

Then, the optimization problem is convex and can be solved by convex optimization tools, such as CVX and MOSEK solvers, which is formulated as

$$\max_{\substack{p_G, y_k, z_k \\ \mathbf{w}_{L,1}, \cdots, \mathbf{w}_{L,K}}} \quad p_G \varphi_r + \frac{p_L A_{L,r}^2 \lambda^2}{16\pi^2 N_L d_{L,r}^4} \sum_{j=1}^{K} y_j \tag{26}$$

$$\text{s.t.} \quad (22), (23), (24), (25), \forall k, (c2) \tag{c3}$$

Note that the beamforming obtained is based on the statistical CSI condition, which is necessary for the long-range, two-layer GEO/LEO SAT ISAC system. Based on the calculated beamforming and power allocation, the detection probability is maximized. Then, in the second stage, the target location estimation method is proposed, which take advantage of the long propagation distance of the two-layer GEO and LEO.

5 Target Location Estimation and CRB Analysis

In the proposed SAT-ISAC scenario, the LEO SAT acts as a cooperate sensing receiver, which receives the echo signal from the GEO-Target link and the LEO SAT reflection. For simplicity, all satellites are assumed to placed in the same plane, i.e. q_r^y, q_G^y, q_L^y is set as 0. The propagation delay of τ_1 and τ_2 shown in (7) can be expressed as $\tau_1 = \frac{d_{G,r}+d_{r,L}}{c}$ and $\tau_2 = \frac{2d_{r,L}}{c}$. With the geometry relationship, the AoD of the SAT to the target can be calculated as

$$\theta_{G,r} = \arctan \frac{q_r^x - q_G^x}{q_G^z - q_r^z}, \theta_{L,r} = \arctan \frac{q_r^x - q_L^x}{q_L^z - q_r^z}. \tag{27}$$

The received signal of the LEO SAT with symbol length M shown in (7) can be expressed as follows

$$\begin{aligned} \mathbf{Y}_L = a_{G,r,L} e^{j2\pi f_d \tau_1} \mathbf{a}^H(\theta_{L,r}) \mathbf{a}^H(\theta_{G,r}) \mathbf{x}_G + \\ a_{r,r,L} e^{j2\pi f_d \tau_2} \mathbf{a}^H(\theta_{L,r}) \mathbf{a}^H(\theta_{L,r}) \mathbf{x}_L + \mathbf{N}_L, \end{aligned} \tag{28}$$

By setting $\begin{matrix} \mathbf{A}(\theta_{L,r}, \theta_{G,r}) = \mathbf{a}^H(\theta_{L,r}) \mathbf{a}^H(\theta_{G,r}) \\ \mathbf{B}(\theta_{L,r}, \theta_{G,r}) = \mathbf{a}^H(\theta_{L,r}) \mathbf{a}^H(\theta_{L,r}) \end{matrix}$, $\mathbf{Y}_L$ can be reformulated as

$$\mathbf{Y}_L = \mathbf{H}_L \alpha + \mathbf{N}_L \tag{29}$$

where $\mathbf{Y}_L \in \mathbb{C}^{N_L \times M}$. $\mathbf{H}_L = [\mathbf{A}(\theta_{L,r}, \theta_{G,r}), \mathbf{B}(\theta_{L,r}, \theta_{G,r})]$. $\alpha = \left[a_{G,r,L} e^{j2\pi f_d \tau_1}, a_{L,r,L} e^{j2\pi f_d \tau_2}\right]^T$.

At the LEO SAT, the target location $\mathbf{q_r}$ can be estimated based on the received echo signal. α can be estimated by calculate the following formula

$$\widehat{\alpha} = \arg\min \|\mathbf{Y}_L - \mathbf{H}_L \alpha\|^2, \tag{30}$$

where $\widehat{\alpha}$ can be computed with the least square (LS) estimation, which is shown as $\widehat{\alpha} = \left(\mathbf{H}_r^H \mathbf{H}_r\right)^{-1} \mathbf{H}_r^H \mathbf{y}_r$. With the estimated $\widehat{\alpha}$, the MLE of the delay and angle can

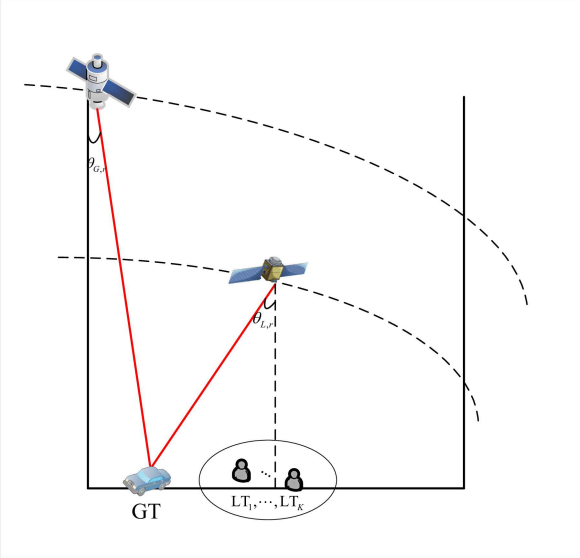


Fig. 2 Example of the target and SAT location of Bistatic ISAC network

be given as

$$(\tau_1, \tau_2, \theta_{L,k}, \theta_{G,k}) = \arg\min \left\| \mathbf{Y}_L - \mathbf{H}_L \widehat{\alpha} \right\|^2 \tag{31}$$

where the related parameters can be obtained by an exhaustive search. As noted in *Remark* 2, the obtained results of $\theta_{G,k}$ cannot be directly used for the target location estimation due to the large propagation distance. Thus, based on the angle and delay parameters $\left\{\widehat{\tau}_1, \widehat{\tau}_2, \widehat{\theta}_{L,r}\right\}$, the target location can be determined according to the geometric relationship illustrated in Fig.2, as follows

$$\begin{aligned} \widehat{q}_r^{\,x} &= q_L^x - \left(\widehat{\tau}_1 - \widehat{\tau}_2\right) c \sin \widehat{\theta}_{L,r} \\ \widehat{q}_r^{\,z} &= q_L^z - \left(\widehat{\tau}_1 - \widehat{\tau}_2\right) c \cos \widehat{\theta}_{L,r} \end{aligned} \tag{32}$$

5.1 CRB for Parameter Estimation

For a target sensing, CRB can be utilized as a theoretical lower bound of the MSE, which is the sensing metric of unbiased estimator [31]. Define $\mu = a_{G,r,L}\mathbf{A}\left(\theta_{L,r}, \theta_{G,r}\right)\mathbf{x}_G + a_{r,r,L}\mathbf{B}\left(\theta_{L,r}, \theta_{L,r}\right)\mathbf{x}_L$, where $\mathbf{A}\left(\theta_{L,r}, \theta_{G,r}\right) = \mathbf{a}\left(\theta_{L,r}\right)\mathbf{a}^H\left(\theta_{G,r}\right)$ and $\mathbf{B}\left(\theta_{L,r}, \theta_{L,r}\right) = \mathbf{a}\left(\theta_{L,r}\right)\mathbf{a}^H\left(\theta_{L,r}\right)$ denote the target response matrices of the from the GEO and the LEO reflection.

Denoting the unknown the parameters $\xi = \{\theta_{G,r}, \theta_{L,r}, a_{G,r,L}, a_{L,r,L}\}$, the FIM $\mathbf{J}_\xi$ can be expressed as

$$\mathbf{J}_\xi = \begin{bmatrix} \mathbf{J}_{\theta,\theta} & \mathbf{J}_{\theta,a} \\ \mathbf{J}_{a,\theta}^T & \mathbf{J}_{a,a} \end{bmatrix}_{4\times 4} \tag{33}$$

where $\mathbf{J}_\xi$ is expressed as $\mathbf{J}_{\theta,\theta} = \begin{bmatrix} J_{\theta_{G,r},\theta_{G,r}} & J_{\theta_{G,r},\theta_{L,r}} \\ J^T_{\theta_{L,r},\theta_{G,r}} & J_{\theta_{L,r},\theta_{L,r}} \end{bmatrix}$. and $[\mathbf{J}]_{i,j} = \frac{2}{\sigma_L^2}\mathrm{Re}\left\{\sum_{t=1}^{T}\frac{\partial\mu^H}{\partial\xi_i}\frac{\partial\mu}{\partial\xi_j}\right\}$. The first-order derivation of $\mathbf{A}(\theta_{L,r},\theta_{G,r}), \mathbf{B}(\theta_{L,r},\theta_{L,r})$ with respect to $\theta_{G,r},\theta_{L,r}$ can be given as

$$\begin{aligned}\dot{\mathbf{A}}_G(\theta_{L,r},\theta_{G,r}) &= \frac{\partial\mathbf{A}(\theta_{L,r},\theta_{G,r})}{\partial\theta_{G,r}} = \mathbf{a}(\theta_{L,r})\dot{\mathbf{a}}^H(\theta_{G,r}) \\ \dot{\mathbf{A}}_L(\theta_{L,r},\theta_{G,r}) &= \frac{\partial\mathbf{A}(\theta_{L,r},\theta_{G,r})}{\theta_{L,r}} = \dot{\mathbf{a}}(\theta_{L,r})\mathbf{a}^H(\theta_{G,r})\end{aligned} \tag{34}$$

and

$$\begin{aligned}\dot{\mathbf{B}}_L(\theta_{L,r}\theta_{L,r}) &= \frac{\partial\mathbf{B}(\theta_{L,r},\theta_{L,r})}{\partial\theta_{L,r}} = \mathbf{a}(\theta_{L,r})\dot{\mathbf{a}}^H(\theta_{L,r}) + \\ &\dot{\mathbf{a}}(\theta_{L,r})\mathbf{a}^H(\theta_{L,r}),\end{aligned} \tag{35}$$

where the derivatives of $\mathbf{a}(\theta_{G,r})$ with respect to $\theta_{G,r}$ is defined as $\dot{\mathbf{a}}(\theta_{G,r}) = \frac{d\mathbf{a}(\theta_{G,r})}{d\theta_{G,r}} = j\frac{2\pi}{\lambda}d_{F,r}\cos\theta_{G,r}\mathrm{diag}(\mathbf{r}_G)\mathbf{a}(\theta_{G,r})$, and $\mathbf{r}_G = [0,...,N_G-1]$ is the Cartesian coordinates of the GEO SAT antenna arrays.

The first-order derivation of μ with respect to $\xi = \{\theta_{G,r},\theta_{L,r},a_{G,r,L},a_{L,r,L}\}$ is expressed as

$$\begin{aligned}&\frac{\partial\mu}{\partial\theta_{G,r}} = a_{G,r,L}\dot{\mathbf{A}}_G(\theta_{L,r},\theta_{G,r})\mathbf{x}_G \\ &\frac{\partial\mu}{\partial\theta_{L,r}} = a_{G,r,L}\dot{\mathbf{A}}_L(\theta_{L,r},\theta_{G,r})\mathbf{x}_G + \\ &a_{r,r,L}\dot{\mathbf{B}}_L(\theta_{L,r},\theta_{L,r})\mathbf{x}_L \\ &\frac{\partial\mu}{\partial a_{G,r,L}} = (1,j)\otimes\mathbf{A}(\theta_{L,r},\theta_{G,r})\mathbf{x}_G \\ &\frac{\partial\mu}{\partial a_{L,r,L}} = (1,j)\otimes\mathbf{B}_L(\theta_{L,r},\theta_{L,r})\mathbf{x}_L\end{aligned} \tag{36}$$

By substituting (36) into (33), the CRB for estimating $\theta_{G,r},\theta_{L,r}$ is expressed as

$$\mathrm{CRB}(\theta_{G,r}) + \mathrm{CRB}(\theta_{L,r}) = \mathrm{tr}\left\{\left(\mathbf{J}_{\theta,\theta} - \mathbf{J}_{\theta,a}\mathbf{J}_{a,a}^{-1}\mathbf{J}_{a,\theta}^T\right)^{-1}\right\} \tag{37}$$

6 Simulation Results

In this section, Monte Carlo simulation are conducted to evaluate the outage performance and the location estimation performance of the proposed two-layer GEO-LEO satellite ISAC system. We model the GEO communication links $g_{G,i}$ using a shadowed-Rician fading channel with parameters $(b_{G,i} = 0.063; m_{G,i} = 1; \Omega_{G,i} = 0.0007)$ for $i \in \{r,1,\cdots,K\}$. The LEO links follow the Rician distribution with parameters $(\kappa_{L,i} = 3, \Omega_{L,i} = 1)$. The other system parameters are listed in Table.1. A 2D coordinate system is used to specify the positions of the GEO, LEO, and target, with coordinates given as (0, 36000) km, (400, 600) km, and (300, 0) km, respectively. LTs are randomly distributed within the coverage area of the LEO satellite.

In Fig.3, we use outage probability to characterize the communication performance of the two-layer satellite communication system versus different CEE values. The transmitting power of the GEO is fixed at 20 dB. The analytical and the asymptotic expressions are derived with the aid of (17) and (18). It can be seen that the theoretical results are close alignment with simulation outcomes, verifying the accuracy of the

Table 1 SYSTEM PARAMETERS

Parameter	Value
$A_{G,i}$	52 dBi
$A_{L,i}$	30 dBi
f_c	12 GHz
$\mathcal{B}$	500 MHz
$\mathcal{T}$	250 K
N_L	4
N_G	5
K	3
σ_i^2	-110 dBm/Hz

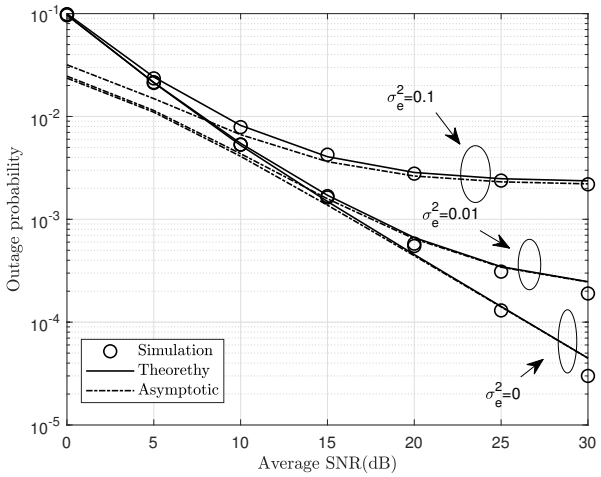


Fig. 3 OP performance versus the LEO SNR with different CEE.

theoretical analysis. Besides, we assume that $\sigma_{e_{G,i}}^2 = \sigma_{e_{L,i}}^2 = \sigma_e^2$ for simplicity. As σ_e^2 increases, the OP degrades. Furthermore, the asymptotic results is adopted to facilitate the optimization of the detection probability. As is shown in Fig.3, the asymptotic results closely match the results with the SNR exceeds 15 dB, demonstrating the accuracy of the asymptotic approximation in the high SNR regime.

Fig.4 illustrates the relationship of the detection probability with different GEO transmitting powers of 0 dB and 20 dB. The detection threshold ξ is set as 17 dB. It can be found that the detection probability is monotonically increasing with the LEO satellite transmitting SNR. Based on the theoretical formulas, it can be found that the increase of p_G decrease the communication performance of the LTs, which illustrates the trade off between communication and sensing.

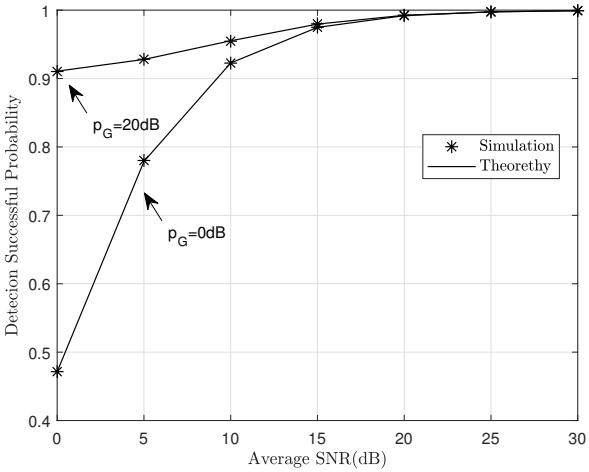


Fig. 4 Detection probability versus LEO and GEO satellite power thresholds.

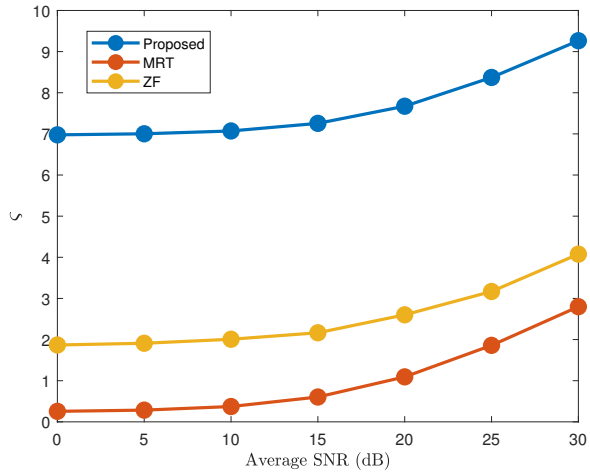


Fig. 5 Detection probability optimization with the comparison of different beamforming algorithms.

Fig. 5 shows the detection threshold with the given P_{MD}=0.1. The optimization problem is solved using the CVX, and the zero-forcing (ZF) and maximum ratio transmission (MRT) schemes are also plotted as benchmarks. As shown in Fig. 5, the proposed algorithm enhances the detection probability, which is essential for reliable target detection in the first stage.

As is shown in the range axis of Fig.7, because the round-trip delay is much longer than the frame of the communication and snesing, each target appears as an isolated pulse, so the delay can be estimated as in pulse radar. Assuming perfect synchronization between the GEO and LEO satellites and both transmit at the initial time, the

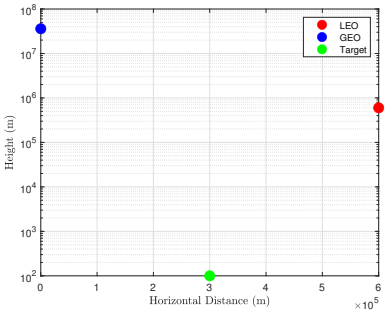


Fig. 6 a. The location of the GEO, LEO SAT and the target

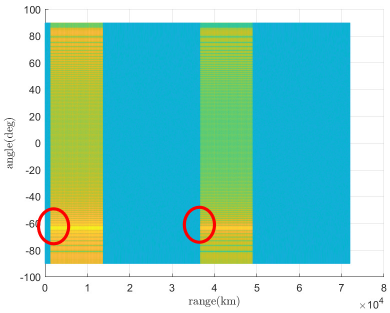


Fig. 7 b. The angle and range 2-D plot

location of the GEO, LEO and target is plotted as Fig.6, where the y-axis is plotted with logarithm value. Since the time taken for the signal to travel from LEO-target-LEO path is much shorter than the time from GEO-target-LEO path, we can consider the left red circle as the τ_2, while the right red one as the τ_1. Since the time delay is on the millisecond scale, it is converted into an equivalent distance for visualization. We then focus on the angle, and the region with high energy corresponds to the direction of arrival (DOA) and angle of arrival (AOA) of the signal.

7 Conclusion

In this paper, we investigate the communication and sensing performance of a two-tier GEO/LEO satellite network. Our study comprises two stages. In the first stage, the LEO radar receiver aims to maximize the detection probability while satisfying the outage probability requirement. We derive closed-form expressions for the detection probability and the outage probability. The proposed optimization problem is solved using a successive convex approximation approach. In the second stage, the LEO satellite estimates the target's location. We utilize time-frequency transmission and a least-squares estimator to obtain the delay and angle, with location estimation achieved through geometric methods. A theoretical lower bound, the CRB, is also derived for comparison. Finally, Monte Carlo simulations are conducted to validate our derivations, demonstrating the efficiency of the proposed SAT-ISAC network in terms of both sensing and communication performance.

References

[1] Cui, Y., Liu, F., Jing, X., Mu, J.: Integrating sensing and communications for ubiquitous iot: Applications, trends, and challenges. IEEE Network **35**(5), 158–167 (2021)

[2] Li, X., Liu, F., Zhou, Z., Zhu, G., Wang, S., Huang, K., Gong, Y.: Integrated sensing, communication, and computation over-the-air: Mimo beamforming design. IEEE Transactions on Wireless Communications **22**(8), 5383–5398 (2023)

[3] Mao, W., Lu, Y., Chi, C.-Y., Ai, B., Zhong, Z., Ding, Z.: Communication-sensing region for cell-free massive mimo isac systems. IEEE Transactions on Wireless Communications (2024)

[4] Liu, Q., Liang, H., Luo, R., Liu, Q.: Energy-efficiency computation offloading strategy in uav aided v2x network with integrated sensing and communication. IEEE Open Journal of the Communications Society **3**, 1337–1346 (2022)

[5] Wang, Z., Mu, X., Liu, Y.: Stars enabled integrated sensing and communications. IEEE transactions on wireless communications **22**(10), 6750–6765 (2023)

[6] Jia, M., Zhang, X., Sun, J., Gu, X., Guo, Q.: Intelligent resource management for satellite and terrestrial spectrum shared networking toward b5g. IEEE Wireless Communications **27**(1), 54–61 (2020)

[7] You, L., Zhu, Y., Qiang, X., Tsinos, C.G., Wang, W., Gao, Z., Ottersten, B.: Ubiquitous integrated sensing and communications for massive mimo leo satellite systems. IEEE Internet of Things Magazine **7**(4), 30–35 (2024)

[8] You, L., Qiang, X., Tsinos, C.G., Liu, F., Wang, W., Gao, X., Ottersten, B.: Beam squint-aware integrated sensing and communications for hybrid massive mimo leo satellite systems. IEEE Journal on Selected Areas in Communications **40**(10), 2994–3009 (2022)

[9] Park, J., Seong, J., Ryu, J., Mao, Y., Shin, W.: Rsma-based bistatic isac framework for leo satellite systems. In: 2024 IEEE International Conference on Communications Workshops (ICC Workshops), pp. 1840–1845 (2024). IEEE

[10] Chang, F., Li, D., Dong, Z.: Performance analysis and system design in geo-leo bistatic sar. IEEE Journal of Selected Topics in Applied Earth Observations and Remote Sensing (2024)

[11] Dong, X., Cui, C., Li, Y., Hu, C.: Geosynchronous spaceborne-airborne bistatic moving target indication system: Performance analysis and configuration design. Remote Sensing **12**(11), 1810 (2020)

[12] Brunner, D., Oliveira, L.G., Muth, C., Mandelli, S., Henninger, M., Diewald, A., Li, Y., Alabd, M.B., Schmalen, L., Zwick, T., et al.: Bistatic ofdm-based isac with over-the-air synchronization: System concept and performance analysis. arXiv preprint arXiv:2405.04962 (2024)

[13] Babu, N., Masouros, C., Papadias, C.B., Eldar, Y.C.: Precoding for multi-cell isac: from coordinated beamforming to coordinated multipoint and bi-static sensing. arXiv preprint arXiv:2402.18387 (2024)

[14] Ding, X., Ren, Z., Lu, H., Zhang, G.: Improving sinr via joint beam and power management for geo and leo spectrum-sharing satellite communication systems.

China Communications **19**(7), 25–36 (2022)

[15] Gu, P., Li, R., Hua, C., Tafazolli, R.: Dynamic cooperative spectrum sharing in a multi-beam leo-geo co-existing satellite system. IEEE Transactions on Wireless Communications **21**(2), 1170–1182 (2021)

[16] Liu, Z., Yin, L., Shin, W., Clerckx, B.: Rate-splitting multiple access for quantized isac leo satellite systems: A max-min fair energy-efficient beam design. IEEE Transactions on Wireless Communications (2024)

[17] Yin, L., Liu, Z., Shankar, M.B., Alaee-Kerahroodi, M., Clerckx, B.: Integrated sensing and communications enabled low earth orbit satellite systems. IEEE Network (2024)

[18] Zheng, Z., Jing, W., Lu, Z., Wu, Q., Zhang, H., Gesbert, D.: Cooperative multi-satellite and multi-ris beamforming: Enhancing leo satcom and mitigating leo-geo intersystem interference. IEEE Journal on Selected Areas in Communications (2024)

[19] Fan, J., Sun, Z., Yue, G., Sun, S.: Performance analysis of integrated sensing and communication by non-orthogonal multiplexing. IEEE Communications Letters (2023)

[20] Abdi, A., Lau, W.C., Alouini, M.-S., Kaveh, M.: A new simple model for land mobile satellite channels: First-and second-order statistics. IEEE Transactions on Wireless Communications **2**(3), 519–528 (2003)

[21] Dwivedi, A.K., Chaudhari, S., Varshney, N., Varshney, P.K.: Performance analysis of leo satellite-based iot networks in the presence of interference. IEEE Internet of Things Journal (2023)

[22] Can, M., Altunbas, I.: Outage probability analysis of rate-splitting multiple-access-based hybrid satellite–terrestrial relay network with relay selection. IEEE Transactions on Aerospace and Electronic Systems **59**(5), 6508–6517 (2023)

[23] Recommendation, I.: Propagation data required for the design of earth-space land mobile telecommunication systems. International Telecommunication Union, 681–686 (2009)

[24] Zheng, Z., Jing, W., Lu, Z., Wu, Q., Zhang, H., Gesbert, D.: Cooperative multi-satellite and multi-ris beamforming: Enhancing leo satcom and mitigating leo-geo intersystem interference. IEEE Journal on Selected Areas in Communications (2024)

[25] Gao, P., Lian, L., Yu, J.: Cooperative isac with direct localization and rate-splitting multiple access communication: A pareto optimization framework. IEEE Journal on Selected Areas in Communications **41**(5), 1496–1515 (2023)

[26] Kell, R.E.: On the derivation of bistatic rcs from monostatic measurements. Proceedings of the IEEE **53**(8), 983–988 (1965)

[27] Hua, M., Wu, Q., He, C., Ma, S., Chen, W.: Joint active and passive beamforming design for irs-aided radar-communication. IEEE Transactions on Wireless Communications **22**(4), 2278–2294 (2022)

[28] Liu, R., Li, M., Liu, Q., Swindlehurst, A.L.: Snr/crb-constrained joint beamforming and reflection designs for ris-isac systems. IEEE Transactions on Wireless Communications (2023)

[29] Teng, T.: Outage probability and ergodic capacity analysis of satellite–terrestrial noma system with mixed rf/mmwave relaying. Physical Communication **57**, 101998 (2023)

[30] Gradshteyn, I.S., Ryzhik, I.M.: Table of Integrals, Series, and Products. Academic press, ??? (2014)

[31] Wei, W., Pang, X., Qin, X., Gong, S., Xing, C., Zhao, N., Niyato, D.: Cramér-rao bound and secure transmission trade-off design for semi-irs-enabled isac. IEEE Transactions on Wireless Communications (2024)